*J. Biochem.* **137**, 601–606 (2005)
DOI: 10.1093/jb/mvi076

# Expression and Characterization of a Baseplate Protein for Bacteriophage Mu, gp44

**Daisuke Kitazawa[1,*], Shigeki Takeda[1,†], Yasuhiro Kageyama[1], Masashi Tomihara[1] and Harumi Fukada[2]**

*[1]Department of Nano-Material Systems, Graduate School of Engineering, Gunma University, 1-5-1 Tenjin-cho, Kiryu, Gunma 376-8515; and [2]Graduate School of Agriculture and Biological Sciences, Osaka Prefecture University, Sakai, Osaka 599-8531*

Received January 19, 2005; accepted March 3, 2005

**The gene product of gene 44 of Mu phage (gp44) is an essential protein for baseplate assembly and has been designated as gpP, a traditional genetic assignment. The function of gp44 during the assembly or infection process is not known. In the present study, we purified the recombinant gp44 and characterized it by analytical ultracentrifugation and differential scanning microcalorimetry. The results indicate that gp44 forms a trimer comprising a complex consisting of the 42 kDa and 40 kDa subunits that had been cleaved in the C-terminal region. Thermodynamic analysis also suggested that the C-terminal region forms a flexible domain.**

**Key words: analytical ultracentrifugation, bacteriophage, differential scanning microcalorimetry, protein assembly.**

Abbreviations: cryoEM, cryo-electron microscopy; DSC, differential scanning calorimetry; gp44, gene product of gene 44; IPTG,isopropyl-1-thio-β-D-galactosidase; PMSF,phenylmethanesulfonyl fluoride; PBS, phosphate buffered saline; PCR, polymerase chain reaction; SDS-PAGE, sodium dodecyl sulfate–polyacrylamide gel electrophoresis.

Bacteriophage Mu is composed of an icosahedral head, a contractile tail with a baseplate, and tail fibers, and belongs to the *Myoviridae* (*1–4*). The Mu phage particle is a genetic delivery vehicle that is equipped for recognition of the host cells and exhibits an exceptionally high efficiency of infection compared with animal viruses. This high efficiency of infection is made possible by the highly elaborate structure of a contractile tail. The tail consists of a slender co-cylindrical part and the baseplate at the end. The gene products of Y, N, P, Q, V, W and R (gpY, gpN, gpP, gpQ, gpV, gpW, and gpR) have been drtermined to be involved in the self-assembly and construction of the Mu phage baseplate (*5*). The structural features and infection process of Mu phage are similar to those of well-known T-even phages. Upon infection of the host bacterium by T4 phage, which is one of the best studied, a conformational change of the baseplate from a "hexagon" to a "star" is observed on electron microscopy (*6*). Concomitantly, the structural change of the baseplate triggers contraction of the sheath that is the outer cylinder of the tail. The mechanisms underlying these structural changes that regulate the molecular interactions are of fundamental interest and remain a frontier of structural biology. Because of their adequate complexity and ease of genetic manipulation, bacteriophages have often been used as a model system for studying a supramolecular structure and its transformation in a biological molecular complex.

Recently, improved structural studies involving crystallography and cryo-electron microscopy (cryoEM) have revealed to details of the structure, assembly mechanism, and infection process of bacteriophages (*7–12*). Extensive genome analysis of phages and host cells has resulted in identification and determination of the relationship of subgroups of many tailed phages (http://spock.genes.nig.ac.jp/~genome/gtop.html). These investigations suggested that there are several strategies for constructing phage structures of which the macro features are similar, since the primary structures of subunits of these phages exhibit very low homology to each other. The T4 phage baseplate, which binds to the host cell membrane and plays an important role in the infection process, is made up of at least 16 types of subunits (*13*). On the other hand, only about eight gene products that exhibit no significant sequence homology to T4 subunits and for which these is little structural information were identified as subunits for the Mu phage baseplate described above (*5*). Therefore, we have purified and investigated a series of structural subunits of Mu gene products in comparing with Mu and T4 phage baseplates. The product of gene 44 of Mu phage (gp44) corresponds to gpP, a traditional genetic assignment, and is an essential protein for baseplate assembly (*5*). We report herein the properties of gp44 in solution determined by analytical ultracentrifugation and differential scanning calorimetry. The results showed that gp44 was a trimer in solution and that its C-terminal region was a relatively flexible structure.

## EXPERIMENTAL PROCEDURES

*Strains and Media*—The Mu phage lysogenic host *Escherichia coli*, MH7213, was kindly denoted by Professor Martha H. Howe (University of Tennessee). *E. coli* XL1-Blue and BL21(DE3)pLysS were used for the construction of an expression plasmid and overexpression of

[*]Present address: Graduate School of Life Sciences, Tohoku University, 2-1-1 Katahira, Aoba-ku, Sendai 980-8577.
[†]To whom correspondence should be addressed. Tel/ Fax: +81-277-30-1434, E-mail: stakeda@bce.gunma-u.ac.jp

 

gp44, respectively. Luria broth comprising 10 g of Bacto Trypton, 5 g of yeast extract, and 10 g of NaCl in 1 liter was used for *E. coli* cultivation.

*Construction of an Expression Plasmid for gp44*—Gene 44 of bacteriophage Mu was amplified by PCR from lysogenic host genome DNA with primers 1 and 2; primer 1, 5′-TTT**GGATCC**CATGAGTAATACCGTCACACTGCGA-3′ (*Bam*HI site in bold) and primer 2, 5′-TTT**CTCGAG**T-TACTCTTTCCACGGCGGC-3′ (*Xho*I site in bold), as well as truncated gene 44 with primers 1 and 3; primer 3, 5′-TTT**CTCGAG**TTAAATACCGCCGTTACTGTCGC-3′ (*Xho*I site in bold). The PCR reaction was performed with 1 unit of KOD plus polymerase (TOYOBO), 5 μM forward and reverse primers, 1 mM $MgCl_2$, 1 mM dNTPs, 0.1 μg genomic DNA, and 1 x buffer supplied by the manufacturer, and a temperature program of 98°C for 15 s, 60°C for 15s, and 68°C for 2min for 30 cycles. The resulting PCR products were purified by 1% agarose gel electrophoresis and cloned into the *Bam*HI–*Xho*I sites of pET17b (Novagen). These expression plasmids were used for transformation of *E. coli* BL21(DE3)pLysS to express gp44 and a deletion mutant that had lost 20 amino acid residues at the C-terminal end. All the DNA sequences were confirmed with a DNA sequencer ABI310 analysis system (Applied Biosystems).

*Protein Expression and Purification*—The transformed *E. coli* cells were grown at 37°C in Luria broth containing 100 μg/ml of ampicillin. Isopropyl-1-thio-β-D-galactosidase (IPTG) was added to a concentration of 1 mM when the optical density at 600 nm reached 0.8. The cells were continuously cultivated for 3 h afterwards, and then harvested by centrifugation at 6,000 rpm for 10 min. The resulting cell pellet was resuspended in 10 mM Tris HCl (pH 8.0), 1 mM EDTA, and then sonicated on ice. Phenylmethanesulfonyl fluoride (PMSF) was added to the crude extract to a final concentration of 1 mM. The extract was centrifuged at 6,000 rpm for 10 min to remove cell debris. The supernatant of the lysed cells was dialyzed twice against 50 mM Tris HCl (pH 8.0). The dialyzed sample was loaded onto a DEAE-Toyopal (Tosho) anion-exchange column (100 ml) equilibrated with the same buffer. Proteins were eluted with linear gradient of NaCl, from 0 to 0.5 M, followed by washing with 50 mM Tris HCl (pH 8.0). The fractions containing gp44 were dialyzed twice against 50 mM MES (pH6.0) and then loaded onto a SP-Toyopearl (Tosho) cation-exchange column (80 ml) equilibrated with the same buffer. Protein elution was performed with a linear gradient of NaCl, from 0 to 0.5 M, followed by washing with 50 mM MES (pH 6.0). The gp44 fractions were concentrated with Amicon ultrafiltration cells with YM-30 filters (Millipore) followed by application to a Sephacryl S-300 (Bio-Rad) gel filtration column (400 ml) equilibrated with 50 mM Tris HCl (pH8.0), 150 mM NaCl. All protein fractions were monitored as to absorption at 280 nm, and subjected to 12.5% SDS-PAGE, which was carried out according to the method described by Laemmli (*14*). The purification procedures described above were carried out at 4°C. The purified gp44 was stored at –80°C. The gp44 concentration was calculated using an extinction coefficient at 280 nm of 1.11, which was estimated from the amino acid composition. For the determination of N-terminal amino acid sequence, the purified gp44 was transferred to a membrane followed by SDS-PAGE. Pieces of the blotted membrane were directly analyzed with a protein sequencer (Applied Biosystems, Procise).

*Analytical Ultracentrifugation*—Analytical ultracentrifugation was performed in phosphate-buffered saline (PBS: 100 mM sodium phosphate, 20 mM potassium phosphate, 140 mM NaCl, pH 7.4), and the same buffer was used as a reference solution. Both sedimentation velocity and sedimentation equilibrium experiments were performed with an Optima XL-I analytical ultracentrifuge (Beckman) with a 4-hole An60Ti rotor at 20°C with standard double-sector centerpieces and quartz windows. The concentration profiles of samples were monitored as to absorbance at 280 nm. The sedimentation velocity experiments were carried out with 0.75 mg/ml of gp44 at a rotor speed of 50,000 rpm. For van Holde-Weischet plots, apparent sedimentation coefficients ($s^*_w$) were estimated from different parts of the sedimentation boundary. The data were plotted on a reciprocal square of time and extrapolated to infinite time by least square fitting in order to determine $s_{20,w}$ (sedimentation coefficient under the standard conditions, 20°C in water). The sedimentation equilibrium experiments were carried out with 0.50 mg/ml of gp44 at a rotor speed of 12,000 rpm. Scans were recorded every 2 h, and the equilibrium of the system was judged by superimposing the last three scans. The partial specific volume, 0.733 $cm^3/g$ was estimated from the amino acid composition of the protein. The partial specific volume, solvent viscosity (1.061 cP), and solvent density (1.016 g/ml) were calculated with the SEDNTERP program (http://www.jphilo.mailway.com/).

*Differential Scanning Calorimetry (DSC)*—Calorimetric measurements were performed with a differential scanning calorimeter, nanoDSC II (CSC, Utah, USA), at a heating rate of 1 K/min. PBS was used as the buffer at pH 7.4. The protein concentration was 2.7 mg/ml. DSC curves were analyzed based on the van't Hoff equation (*15*).

## RESULTS

*Purification of gp44*—We successfully expressed gp44 in soluble fractions by using a T7 polymerase expression system, and purified it by anion-exchange chromatogra-

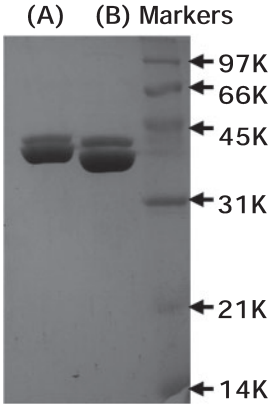


Fig. 1. **SDS-PAGE analysis of purified gp44.** (A) full-length gp44 and (B) C-terminal truncated gp44.

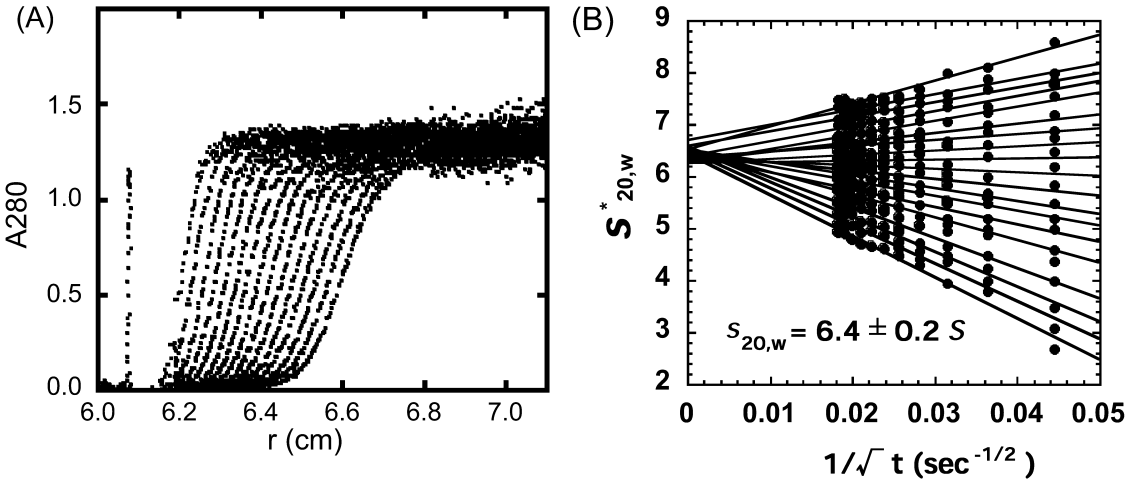


Fig. 2. **Sedimentation velocity experiments on gp44.** (A) The moving boundaries were monitored as to absorbance of 280 nm and at a rotor speed of 50,000 rpm. The protein concentration was 0.75 mg/ml. Scans were recorded every 2 h. (B) The van Holde-Weischet analysis. The $s_{20,w}$ was determined to be 6.4 ± 0.2 *S*. The analysis indicated that a specimen exhibited only a single species.

phy, cation-exchange chromatography, and gel filtration. The purified fraction gave a doublet band on SDS-PAGE (Fig. 1). The estimated molecular mass values for these bands were 42 kDa and 40 kDa. Preliminary mass spectrometric analysis gave almost the same results (Y. Kondou *et al*., unpublished data). Since the molecular weight of full-length gp44 estimated from the nucleotide sequence was 41.8 kDa, we supposed that the 42 kDa material was full-length gp44 and the 40 kDa one was a processed form. To confirm the heterogeneity of the N-terminal regions of these two species, they were analyzed by Edman degradation. Both the determined amino-terminal sequences were SNTVTLRAD, which is identical to that of gp44, as deduced from the nucleotide sequences (*16*). We also purified a truncated gp44, 20 residues have been removed at the C-terminal end by genetic engineering. This truncated gp44 also gave a doublet band on SDS-PAGE and had the same N-terminal sequence (Fig. 1).

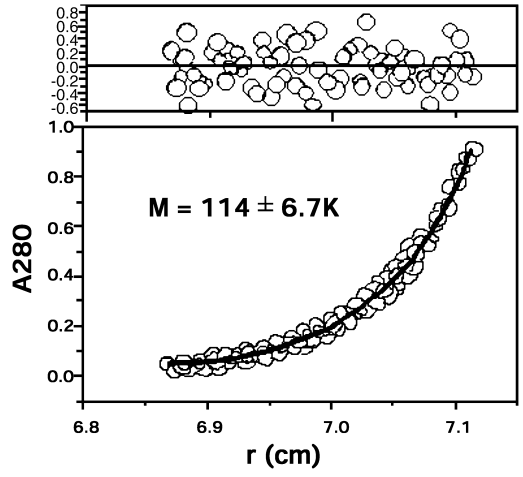


Fig. 3. **Sedimentation equilibrium experiments on gp44.** The rotor speed was 12,000 rpm and the protein concentration was 0.5 mg/ml. The obtained molecular weight was 114 ± 6.7 kDa.

*Analytical Ultracentrifugation*—To determine the oligomerization state of gp44 in solution, the molecular weight of the protein was determined by analytical ultracentrifugation. First, sedimentation velocity analysis was carried out to examine the homogeneity of the purified protein, since the purified fraction comprised of full-length 42 kDa and processed 40 kDa subunits. A single symmetric boundary was observed (Fig. 2), which indicated that the 42 kDa and 40 kDa subunits formed a single oligomeric species. Using these data, we performed van Holde-Weishet ploting to determine the sedimentation coefficient and to confirm the homogeneity of the sample in solution. The fact that all six *y* intercepts exhibited fine convergence also indicated that the gp44 solution contained a single protein species. The sedimentation coefficient, $s_{20,w}$, was calculated to be 6.4 ± 0.2 *S* from the average of *y* intercepts. Sedimentation equilibrium revealed that the molecular weight was 114 ± 6.7 kDa (Fig. 3). Judging from the calculated molecular weight of 42 kDa or 40 kDa for a gp44 subunit expected from the nucleotide sequence and the results of SDS-PAGE, gp44 formed a trimer.

*DSC Analysis of Wild Type and C-Terminal Truncated gp44*—The wild type gp44 and the C-terminal truncated gp44 mutant were analyzed by DSC to determine the properties of the C-terminal region of gp44. DSC measurements revealed that both samples gave a single symmetric peak as shown in Fig. 4. The total area under the DSC curve for the C-terminal truncated mutant was smaller compared to that for the wild type. The peak temperature for the mutant was 69°C, *i.e.*, 1 K higher than that for the wild type. This peak shift seemed to indicate that the C-terminal deletion resulted in slight stabilization of the remaining portion.

The thermal denaturation was found to be accompanied by precipitation of the sample protein in the case of both the wild type and mutant, indicating that these processes are irreversible and that thermodynamic analysis is only applicable to a limited extent. However, it has been reported that for some proteins having domain structures, the observed DSC curves can be quantita-

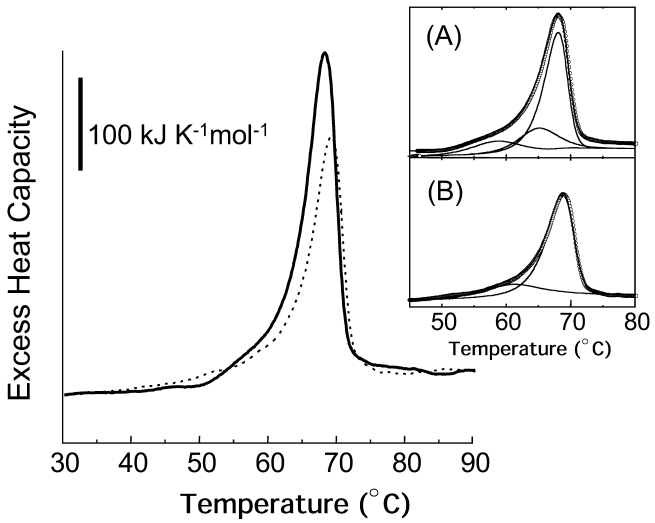


Fig. 4. **DSC measurements of gp44. DSC curves for the thermal transition of the wild type gp44 (solid line) and the mutant devoid of C-terminal 20 residues (dashed line).** The insets show the results of curve resolution based on the van't Hoff equation. (A) The wild type gp44, (B) the deletion mutant. Open circles, the observed DSC data; thin lines, component curves; thick lines, sums of component contributions.

tively and successfully resolved into some components that correspond to the thermal unfolding of each domain (*17*, *18*). Considering this, the curve resolution technique was employed in the present study and the results obtained are shown in the insets in Fig. 4. Assuming that the trimer proteins undergo dissociation into denatured monomers in at the final step of denaturation, the observed DSC curves were resolved into 3 and 2 components for the wild type (Fig. 4A) and C-terminal truncated mutant (Fig. 4B), respectively. From Fig. 4 it is clear that the sum of the each component in thick lines well fits the observed DSC curves (open circles). Thus the result of curve resolution strongly suggested that the wild type protein consisted of three domains, each of which showed an independent two-state transition, while the thermal denaturation of the truncated mutant proceeded *via* two independent two-state transitions. The transition temperature, $t_m$, and the corresponding enthalpy change, $\Delta H$ obtained for the each component on the curve resolution are summarized in Table 1.

## DISCUSSION

During expression and the purification process, we found that gp44 gave two bands on SDS-PAGE corresponding to 42 kDa and 40 kDa. In addition, on SDS-PAGE of native Mu tails, we found the putative gp44 bands around 42 kDa were also a doublet (*19*). Therefore, we consider that a part of the gp44 is processed in Mu phage particles. To investigate the heterogeneity of gp44 at the N- and C-termini, we performed N-terminus sequencing and C-terminus deletion experiments. N-terminal sequencing clearly indicated both materials, 42 kDa and 40 kDa, had the same N-terminal and started from the second residue, serine. In general, the N-terminal methionine residue is cleaved off by *E. coli* amino peptidase that removes the initial methionine when the side chain of the second residue is small and has no charge (*20*, *21*). The C-terminal deletion mutant also gave two bands on SDS-PAGE (Fig. 1) and had the same N-terminal sequence as the wild type. We conclude that a part in gp44 is processed at a specific C-terminal region and that its cleavage site possibly changes with a minor C-terminal sequence modification. Analytical ultracentrifugation was performed to confirm the protein purity and molecular weight of gp44 in solution. Sedimentation velocity experiments and van Holde-Weischet analysis indicated that a specimen exhibited single species in spite of heterogeneity as to the C-terminus. Since sedimentation equilibrium experiments showed gp44 forms a trimer, the trimer consists of mixture of 42 kDa and 40 kDa subunits. We have already obtained single crystals of gp44 for X-ray crystallography (*22*). The fact that crystals of gp44 also gave doublet bands on SDS-PAGE was consistent with this consideration (data not shown). We roughly estimated the stoichiometry of the 42 kDa and 40 kDa subunits from the band densities on SDS-PAGE (Fig. 1) and concluded that approximately 30% of gp44 was 42 kDa. This suggests that a trimer of gp44 consists of one 42 kDa and two 40 kDa subunits.

The other problems were how many thermodynamically independent domains gp44 has, and to assign the thermal transitions to individual structural regions. According to the results of DSC curve resolution, the wild type gp44 exhibits three independent components in the thermal denaturation process, suggesting that gp44 consists of three thermodynamically distinguishable domains. The major peak at the transition temperature of 67.5°C exhibited an enthalpy change that was four times larger than the other two transitions at 57.4°C and 64.7°C. This showed good agreement on curve resolution analysis when this process was assumed to include dissociation of the trimer into three monomers. The peak at 67.5°C was, therefore, assigned to the dissociation of subunits into monomers. These indications suggest that the thermally induced denaturation of gp44 proceeds via three transition states in the order of the native trimer, two types of intermediate trimer, and three dissociated and denatured monomers, the dissociation and denaturation taking place simultaneously. It is a valid objection that the wild type transitions at 57.4°C and 67.5°C correspond to those of the C-terminal truncated mutant at 60.1°C and 68.1°C, respectively, and that these transi-

Table 1. **The transition temperatures and enthalpy changes for unfolding of the resolved components of gp44 at pH 7.4.**

| Protein | Component 1 | | Component 2 | | Component 3 | |
|---|---|---|---|---|---|---|
| | $t_m$/°C | $\Delta H$/kJ mol$^{-1}$ | $t_m$/°C | $\Delta H$/kJ mol$^{-1}$ | $t_m$/°C | $\Delta H$/kJ mol$^{-1}$ |
| Wild gp44 | 57.4 | 330 | 64.7 | 467 | 67.5 | 1,450 |
| Mutant | 60.1 | 312 | – | – | 68.1 | 1,300 |

tions originate from the same domain, since the transition temperatures and enthalpy changes are very similar. Therefore, we conclude that the remaining transition at 64.7°C can be assigned to a C-terminal domain. This consideration and the fact that the C-terminal domain is cleaved in the processing process suggest that the C-terminal domain has a flexible structure. The relationship between the flexible structure in a C-terminal region and its importance for assembly and/or structural change of the supramolecular structure has been reported for several proteins. For example, a C-terminal region of bacterial flagellin is protease-sensitive, and is involved in the assembly and conformational switching of flagellar filaments (*23*). The C-terminal region of the T4 phage sheath subunit, gp18, is a protease-sensitive domain and is considered to assume a somewhat flexible structure. The tail sheath contracts upon adsorption to the host bacterium. It was surmised that the flexible structure of gp18 would play an important role in sheath contraction and gross conformational change of the sheath (*24*). The T4 baseplate changes in structure from a hexagon to a star upon infection (*11*). We speculate that the Mu baseplate has also the ability to change its structure during the infection process, and that the C-terminal region of gp44 is responsible for baseplate transformation and subunit rearrangement during the infection process.

To consider another thermodynamical region corresponding to the transition temperatures of 57.4°C for the wild type and 60.1°C for the C-terminal truncated mutant, respectively, we examined the homology of the primary structure in a public database. Recent growth in nucleotide sequencing capability has renewed interest in bacteriophage diversity. Mu-like prophages have recently been discovered in several bacterial genomes. We found 14 protein sequences that were significantly homologous with gp44 in the GTOP database (http://spock.genes.nig.ac.jp/~genome/gtop.html). All of these proteins were thought to be subunits of Mu-like phages or putative subunits of lysogenic phages in several bacterial genomes. Multiple sequence alignment of these proteins indicated that there is only one region that has more than 5 residues inserted or deleted around residue 220 (http://spock.genes.nig.ac.jp/~genome/cgi-bin/bltpro.cgi?org=bpmu0&tar=BLTORG&id=AAF01122.1). It is possible to surmise that this region accepts a valuable length, probably because of its fragile structure. To confirm this consideration, we constructed a deletion mutant devoid of Lys210–Arg231 and tried to purify it. But this deletion mutant was not expressed very well and was suspected to easily undergo degradation in the cells. X-ray crystallization of gp44 is now underway and will be reported very soon (*22*). The results will clarify gp44's structure, stability, function, and assembly mechanism.

We thank Professor Martha H. Howe (University of Tennessee) for the Mu phage strains and Professor Fumio Arisaka (Tokyo Institute of Technology) for his great help in the analytical ultracentrifugation. We also thank Professor Tomitake Tsukihara and Doctor Yohei Kondou (Institute for Protein Research, Osaka University) for the fruitful discussions. This work was supported by Grants-in-Aid from the Gunma University Foundation for Science and Technology, the Suzuki Foundation, and the Ministry of Education, Science, Sports, and Culture of Japan to S.T.

REFERENCES

1. Inman, R.B., Schnos, M., and Howe, M. (1976) Location of the "variable end" of Mu DNA within the bacteriophage particle. *Virology* **72**, 393–401
2. Admiraal, G., Mellema, J.E., Grundy, F.J., and Howe, M.M. (1976) The structure of the contractile sheath of bacteriophage Mu: Morphogenetic structures present in lysates of amber mutants of bacteriophage Mu. *J. Ultrastruct. Res.: Virology* **56**, 48–64
3. Grundy, F.J. and Howe, M.M. (1984) Involvement of the invertible G segment in bacteriophage mu tail fiber biosynthesis. *Virology* **134**, 296–317
4. To, C.M., Eisenstark, A., and Toreci, H. (1966) Structure of mutator phage Mu1 of *Escherichia coli*. *J. Ultrastruct. Res.* **14**, 441–448
5. Grundy, F.J. and Howe, M.M. (1985) Morphogenetic structures present in lysates of amber mutants of bacteriophage Mu. *Virology* **143**, 485–504
6. Crowther, R.A., Lenk, E.V., Kikuchi, Y., and King, J. (1977) Molecular reorganization in the hexagon to star transition of the baseplate of bacteriophage T4. *J. Mol. Biol.* **116**, 489–523
7. Kanamaru, S., Leiman, P.G., Kostyuchenko, V.A., Chipman, P.R., Mesyanzhinov, V.V., Arisaka, F., and Rossmann, M.G. (2002) Structure of the cell-puncturing device of bacteriophage T4. *Nature* **415**, 553–557
8. Leiman, P.G., Kanamaru, S., Mesyanzhinov, V.V., Arisaka, F., and Rossmann, M.G. (2003) Structure and morphogenesis of bacteriophage T4. *Cell. Mol. Life Sci.* **60**, 2356–2370
9. Kostyuchenko, V.A., Leiman, P.G., Chipman, P.R., Kanamaru, S., van Raaij, M.J., Arisaka, F., Mesyanzhinov, V.V., and Rossmann, M.G. (2003) Three-dimensional structure of bacteriophage T4 baseplate. *Nat. Struct. Biol.* **10**, 688–693
10. Arisaka, F., Kanamaru, S., Leiman, P., and Rossmann, M.G. (2003) The tail lysozyme complex of bacteriophage T4. *Int. J. Biochem. Cell Biol.* **35**, 16–21
11. Leiman, P.G., Chipman, P.R., Kostyuchenko, V.A., Mesyanzhinov, V.V., and Rossmann, M.G. (2004) Three-dimensional rearrangement of proteins in the tail of bacteriophage T4 on infection of its host. *Cell* **118**, 419–429
12. Rossmann, M.G., Mesyanzhinov, V.V., Arisaka, F., and Leiman, P.G. (2004) The bacteriophage T4 DNA injection machine. *Curr. Opin. Struct. Biol.* **14**, 171–180
13. Kikuchi, Y. and King, J. (1975) Genetic control of bacteriophage T4 baseplate morphogenesis. III. Formation of the central plug and overall assembly pathway. *J. Mol. Biol.* **99**, 695–716
14. Laemmli, U.K. (1970) Cleavage of structural proteins during the assembly of the head of bacteriophage T4. *Nature* **227**, 680–685
15. Kitamura, S. and Sturtevant, J.M. (1989) A scanning calorimetric study of the thermal denaturation of the lysozyme of phage T4 and the Arg 96—His mutant form thereof. *Biochemistry* **28**, 3788–3792
16. Morgan, G.J., Hatfull, G.F., Casjens, S., and Hendrix, R.W. (2002) Bacteriophage Mu genome sequence: analysis and comparison with Mu-like prophages in *Haemophilus*, *Neisseria* and *Deinococcus*. *J. Mol. Biol.* **317**, 337–359
17. Tanaka, A., Fukada, H., and Takahashi, K. (1995) Differential scanning calorimetric studies on the domain structure of *Aspergillus* glucoamylase. *J. Biochem.* **117**, 1024–1028
18. Coutinho, P.M. and Reilly, P.J. (1997) Glucoamylase structural, functional, and evolutionary relationships. *Proteins* **29**, 334–347
19. Takeda, S., Sasaki, T., Ritani, A., Howe, M.M., and Arisaka, F. (1998) Discovery of the tail tube gene of bacteriophage Mu and sequence analysis of the sheath and tube genes. *Biochim. Biophys. Acta* **1399**, 88–92
20. Ben-Bassat, A., Bauer, K., Chang, S.Y., Myambo, K., Boosman, A., and Chang, S. (1987) Processing of the initiation

methionine from proteins: properties of the *Escherichia coli* methionine aminopeptidase and its gene structure. *J. Bacteriol.* **169**, 751–757
21. Sherman, F., Stewart, J.W., and Tsunasawa, S. (1985) Methionine or not methionine at the beginning of a protein. *Bioessays* **3**, 27–31
22. Kondou, Y., Kitazawa, D, Takeda, S., Yamashita, E., Mizuguchi, M., Kawano, K., and Tsukihara, T. (2005) Crystallization and preliminary X-ray analysis of gene product 44 from bacteriophage Mu. *Acta Cryst. F* **61**, 104–105
23. Samatey, F.A., Imada, K., Nagashima, S., Vonderviszt, F., Kumasaka, T., Yamamoto, M., and Namba, K. (2001) Structure of the bacterial flagellar protofilament and implications for a switch for supercoiling. *Nature* **410**, 331–337
24. Takeda, S., Arisaka, F., Ishii, S., and Kyogoku, Y. (1990) Structural studies of the contractile tail sheath protein of bacteriophage T4. 1. Conformational change of the tail sheath upon contraction as probed by differential chemical modification. *Biochemistry* **29**, 5050–5056